Dielectric Studies of Hyperbranched Aromatic Polyamide and Polyamide-6,6 Blends

C. Hakme,[1] I. Stevenson,[1] R. Fulchiron,[1] G. Seytre,[1] F. Clement,[2] L. Odoni,[2] S. Rochat,[2] J. Varlet[2]

[1]*Laboratoire des Matériaux Polymères et des Biomatériaux, UMR CNRS 5627,Bât. ISTIL, Université Claude Bernard Lyon 1, 15, Bd. Latarjet, 69622 Villeurbanne Cedex, France*
[2]*CRTL, Rhodia Recherches, 85 rue des Frères Perret, BP62 69192 St-Fons Cedex, France*

Received 12 May 2004; accepted 4 January 2005
DOI 10.1002/app.21907
Published online in Wiley InterScience (www.interscience.wiley.com).

ABSTRACT: The objective of this work was to study the interactions between polyamide-6,6 (PA-6,6) and hyperbranched (HB) polyamide with different functional end groups. The investigation focused on the thermal, dielectric, and viscoelastic properties of two kinds of HB polyamides, with amine and alkyl end groups, prepared by a one-pot process, in a polyamide-6,6 matrix. Thermal analysis (by TGA and DSC) allowed us to observe decomposition and glass-transition temperatures of these polymers. The melting point, crystallization temperature, and crystallinity ratio remained practically independent of HB content. Dielectric relaxation spectroscopy (DRS) showed two secondary relaxation (γ and β) and one primary (α) relaxation in the HB polymers and in the blends similar to those observed in polyamide-6,6 with comparable activation energies and distribution parameters. An increase of the glass-transition temperature was observed, showing a reinforcement of the polymer matrix and a decrease of the molecular mobility of the polyamide chains when the percentage of amine-terminated HB polyamide increased in the matrix. DRS results found on the alkyl-terminated HB polymer blend were indistinct from those of the polyamide-6,6 matrix. Viscoelastic experiments confirmed the results observed in DRS. © 2005 Wiley Periodicals, Inc. J Appl Polym Sci 97: 1522–1537, 2005

Key words: dielectric properties; viscoelastic properties; hyperbranched; polyamides; relaxation

INTRODUCTION

Hyperbranched polymers are new materials resulting from macromolecular synthesis and have lately been part of one of the most interesting fields in polymer science; they have an exceptional molecular architecture (ramified structure), which confers very particular properties compared to those of similar linear polymers, such as viscosity, melting point, and reactivity. Dozens of patents have recently been filed on the synthesis of dendritic polymers of varying chemistries. However, the exploitation of dendritic polymer technology is still undeveloped because of the limited availability and the expensive synthesis of these materials. Therefore the development of hyperbranched polymers seems to have a better industrial future than that of dendrimer molecules because they are less expensive to produce and have a wider range of applications.

In addition, the large number of terminal functional groups contained in these molecules control the properties of the resulting polymers such as solubility and reactivity.[1–8] Hyperbranched polymers are often synthesized by a one-pot polymerization of AB_x-type monomers; this process consists of an activation of carboxyl groups as well as a condensation with an AB_2 monomer, finally attaining a highly irregular structure.[2,9] These polymers are composed of terminal, linear, and dendritic units that are distinguished by the number of unreacted functional groups in the unit.[10] The degree of branching (DB) is largely used as a parameter to indicate the architecture of hyperbranched polymers[10] and is defined as $DB = (D + T)/(D + T + L)$, where D is the number of dendritic units, T is the number of terminal units, and L is the number of linear units. Frey et al.[7] reported that the one-pot polymerization of AB_2-type monomers statistically gives a degree of branching of 0.5 when the reactivity of functional groups in each unit is identical.[7,11,12]

Aromatic polyamides have been well established as high-performance polymers because of their excellent thermal, mechanical, and chemical properties. Hyperbranched macromolecules are renowned to have a higher solubility and a lower viscosity by an order of magnitude than those of their linear analogues.[1,9,13–15] This low viscosity derives from the spherical shapes of these polymers that make them less likely to be entangled.

Correspondence to: I. Stevenson (isabelle.stevenson@univ-lyon1.fr).
Contract grant sponsor: CRL, Rhodia St-Fons, France.

Hyperbranched polyamides have been reported soluble in organic solvents, even if the rigidity of the main chains of their linear analogues prevents the latter from being soluble.[10] The investigation of glass-transition temperature (T_g) in hyperbranched polymers has correlated T_g with the number of monomer units, number of chain ends, molecular weight, and chain-end composition.[16–18] Generally, the variation of T_g with molecular weight correlates well with theoretical predictions, although the value of T_g is substantially affected by the nature of the chain ends and internal monomer units.[19] Finally, the specificity of hyperbranched molecules is to have a high density of function per molecule compared to that of linear polymers.

Studies on hyperbranched polymer/thermoplastic blends have been limited to miscible and/or nonreactive systems.[20–22] However, no studies have directly been intended for assessing the use of dendritic polymers as components in a polymer blend with a controlled morphology designed to improve the mechanical performance. The functional terminal groups are numerous on these molecules, thus making them good candidates for reactively compatibilized blends, in which coreactive moieties on the dendritic polymer and matrix polymer would form compatibilizers in their usual place during processing. These compatibilizers act to reduce the interfacial tension in a multiphase blend,[23–25] to increase the interfacial adhesion, and to stabilize the dispersion against coarsening during processing or subsequent forming operations, and generally enhance blend formation. In addition, the low melting viscosity in the dendritic polymers confers an advantage that may counterbalance the increase in viscosity that is often encountered during reactive blending as a result of copolymer formation and the associated molecular weight buildup.[26–28] Thus, the dendritic polymers properties are likely to modify the rheological behavior of the matrix in which these hyperbranched molecules are blended so they are an ideal choice for thermoplastic blend modifiers because they can improve both properties and processability. This work is mostly aimed at investigating the incorporation of hyperbranched polymers into a thermoplastic system. Studies have focused on the thermal viscoelastic and electrical properties of these polymers.

Dielectric relaxation spectroscopy (DRS) investigates and explains different relaxation processes (α-, β-, and γ-relaxations) of hyperbranched and dendritic polymers. For example, dielectric spectroscopy on hyperbranched polyesters, with the same backbone but different terminal groups, allows determination of glass transitions (α-relaxation) that match with those obtained in DSC measurements and dynamic mechanical analyses.[29] This spectroscopy also distinguishes different β- and γ-relaxation processes for the terminal ester and hydroxyl groups. Thus, Zhu et al.[30] studied the dielectric relaxations in a hyperbranched polyester with terminal hydroxyl groups and reported an effect of generation number. Stuhn et al.[31,32] applied dielectric spectroscopy on carbosilane dendrimers with flexible perfluorinated and mesogenic end groups to study the possible smectic and nematic state and the transitions of these highly flexible dendritic molecules. Emran et al.[33] also presented an example for ester-terminated, amide-based dendrimers, in addition to the dielectrical analyzed carbosilane dendrimers. The relaxation rate dependency of the glass transition of these polymers was characterized by the VFT (verification front-end tool) formalism.[34–36] These hyperbranched polymers show a secondary relaxation with an Arrhenius-type temperature dependency. Dantras et al.[37] studied the β-relaxation in phosphorus-containing dendrimers using thermally stimulated current (TSC) and broadband dielectric spectroscopy, with the aim of analyzing the molecular mobility evolution upon increasing generation. In summary, the application of DRS on hyperbranched polyamide can foster a better understanding of molecular dynamics.

Properties of polyamide-6,6 are well known in the literature and detailed information can be found in McCrum et al.[38] and Hedvig et al.[39] More recently, Steeman and Maurer[40] compared the dielectric properties of polyamide-4,6 with the dynamic dielectric properties of commercial polyamide-6,6. Havriliak et al.[41] were also interested in the dielectric and mechanical relaxation of polyamides, among other polymers. Kremer and Schönhals[42] give a review of articles on dielectric analysis of polyamides in their book. Generally, three polarization mechanisms related to molecular motions are observed.

1. At lower temperatures (between −140 and −100°C) a weak polarization mechanism is found, attributed to local motion of chain segments, mainly alkyl segments, located between the interchain hydrogen bonds.
2. Close to −50°C a polarization mechanism, related to a mechanism of rotation of the amide bonds together with water molecules that are bonded to them, is observed. The principal relaxation is observed at higher temperatures (50–70°C).
3. Above this relaxation and at higher temperatures, materials (such as polyamide-6,6) become electrically conductive and show a sharp increase in dielectric constant,[43] which is thought to be attributed to an interfacial [or Maxwell–Wagner–Sillars (MWS)] polarization process as a result of trapping of free-charge carriers at boundaries between crystalline and amorphous phases. The addition of hyperbranched polyamide with different terminations in a matrix with different polarity may affect this interfacial polarization, which can be detected by DRS.

EXPERIMENTAL

Materials

This work contains a study of hyperbranched polyamides prepared by a "one-pot" polymerization. Details of synthesis of these polymers are described elsewhere.[44,45] Two types of chain ends are considered: (1) amine, polymer A or aliphatic end groups (C_{16}); (2) polymer B [see Fig. 1(a) and (b)]. In the case of the amine-terminated hyperbranched polymers [see Fig. 1(a)], the molar proportion of the different constituents are as follows: 1 mol of tris(amino 2 ethyl)amine N $\{[(CH_2)_2NH_2]_3\}$ as the core molecule, 6 mol of caprolactam as spacing unit, and 6 mol of 3,5-diaminobenzoic acid as branching unit; no chain terminator is used. In the case of the alkyl-terminated hyperbranched polymers [see Fig. 1(b)], the molar proportion of the different constituents are 1 mol of trimesic acid as the core molecule, 6 mol of amino-isophthalic acid as branching unit, 6 mol of caprolactam spacing unit, and, in this case, a chain terminator is used (i.e., 9 mol of hexadecylamine).

Pellets of polyamide-6,6 and its blends, prepared by twin-screw extrusion, with hyperbranched aromatic polyamide were provided by Rhodia Research Center (CRL) in Lyon, France. Dielectric analyses require the processing of homogeneous films, so polyamide pellets were pressed at 300°C between two Teflon sheets. Films having a thickness of nearly 150 μm were obtained. Two kinds of blends were investigated: the polyamide-6,6 blended with amine-terminated HB and the polyamide-6,6 blended with alkyl-terminated HB with different percentages. The following blends were investigated:

- C: Polyamide-6,6 (reference)
- D: Polyamide-6,6 with 2% of amine-terminated hyperbranched aromatic polyamide
- E: Polyamide-6,6 with 5% of amine-terminated hyperbranched aromatic polyamide
- F: Polyamide-6,6 with 5% of alkyl-terminated hyperbranched aromatic polyamide
- G: Polyamide-6,6 with 10% of alkyl-terminated hyperbranched aromatic polyamide

Molecular weights were measured by gel permeation chromatography (GPC) in *N,N'*-dimethylacetamide. A small amount of LiBr was added to the solution to promote the breaking of hydrogen bonds. The calibration was done using polystyrene references and thus the weight-average molecular mass (M_w) given are polystyrene-equivalent values: M_w values for pure hyperbranched polymers are 9500 g/mol for polymer A (amine-terminated hyperbranched polymer) and 7750 g/mol for polymer B (aliphatic-terminated hyperbranched polymer). The average molecular weight of polyamide-6,6 used for the blends measured by the same method (polystyrene references) give the following values: M_n = 43,000 g/mol; M_w = 75,750 g/mol; M_z = 114,250 g/mol. It can thus be seen that the pure hyperbranched polymers are characteristically small molecules compared to polyamide-6,6. However, they are more compact than PA-6,6 but they are probably three times heavier than a linear PA-6,6 with an equivalent steric hindrance.

Measurements

DSC was carried out by use of a DSC 2920 apparatus (TA Instruments, New Castle, DE), at a heating rate of 10°C/min under a flow of helium. Samples under investigation were pellets and weighed approximately 10–15 mg. The crystallinity was calculated using the ΔH_∞ value of polyamide-6,6 (255.8 J/g)[46] and the amount of hyperbranched polymer in the blends was taken into account. Glass-transition temperatures were measured at the midpoint and during the second run. Step-scan measurements were carried out on a Pyris-1 modulated DSC apparatus (Perkin–Elmer Cetus Instruments, Norwalk, CT). The powder was introduced to an aluminum pan with a pinhole. Measurement conditions were as follows: isotherm step time = 30 s, anisotherm scan time = 30 s, anisotherm scan rate: 4 K/mn, and sample weight = 10 mg.

Thermogravimetric analysis (TGA) was performed with a TA Instruments TGA 2950 instrument, at a heating rate of 10°C/min under helium flow for samples of about 10 mg. Infrared (FTIR) spectra were recorded on a Perkin–Elmer 1760X instrument, either in the powder form (KBr discs) or as films (PA-6,6 or blends), using ATR accessory (KRS-5 crystal). Dielectric measurements were recorded using a Novocontrol dielectric spectrometer (Novocontrol GmbH, Hundsangen, Germany) covering a large domain of frequency (10^{-1} to 10^6 Hz; thus 22 frequencies in total, constituting three frequencies per decade). Experiments were carried out between −140 and 220°C and samples were dried before analysis for 2 h *in situ* at 110°C. Dielectric spectra were recorded isothermally during a frequency scan performed every 3°C. Hyperbranched molecules (polymers A and B) were available as powders. It was not possible to produce films with these powders because they were brittle and difficult to handle. However, it was possible to directly study the powder in a specially designed cell for powder. Thus, the powder was kept between two specific electrodes (23 mm in diameter) with a 40-μm silica spacer. For data analysis, curves were fitted using a single Havriliak–Negami[47] (H.N.) function with no additional conductivity term for the secondary relaxations but subtracting the conductivity term for the α-relaxation.

In the frequency domain, the H.N. equation is expressed as follows:

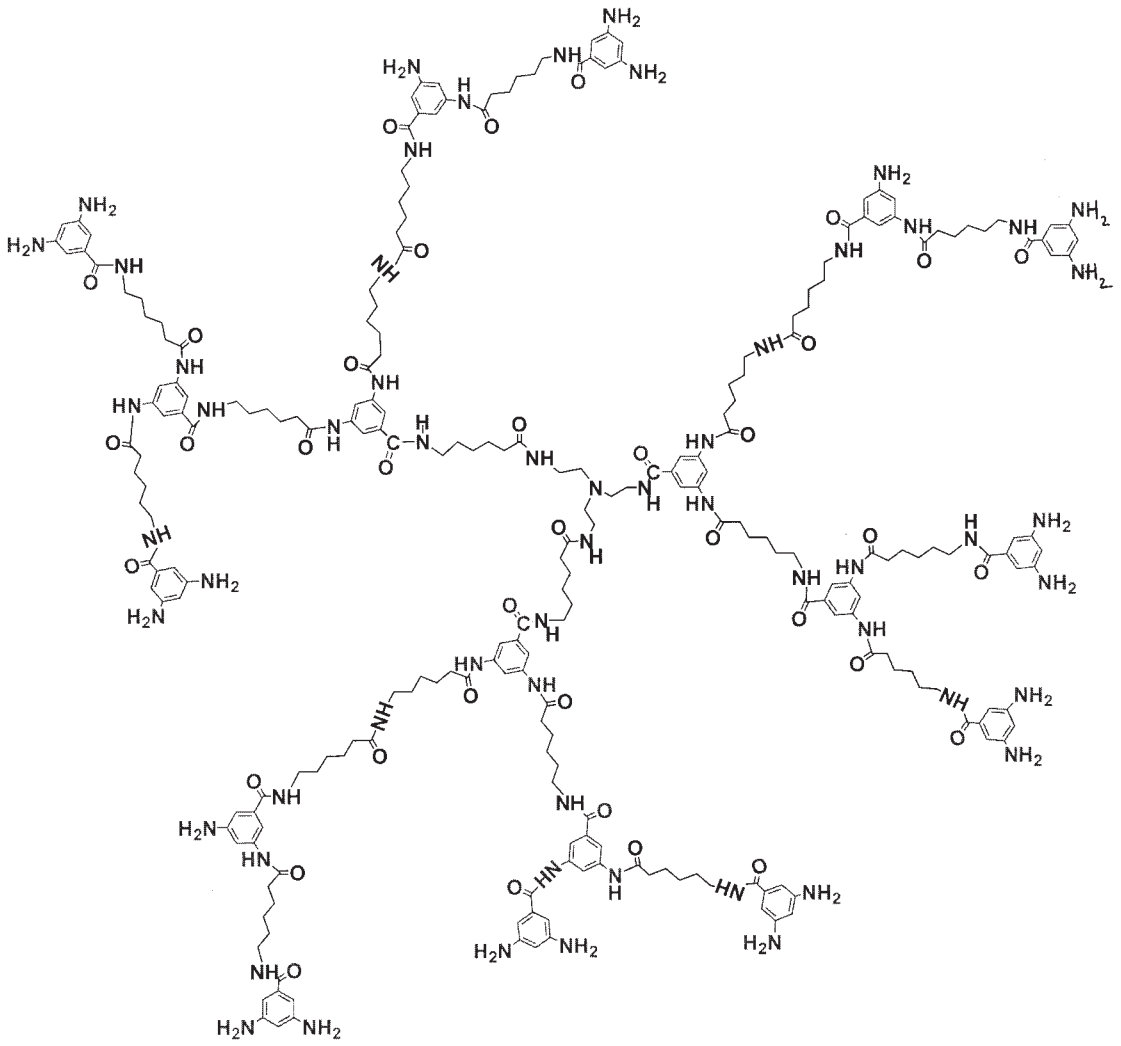

(a)

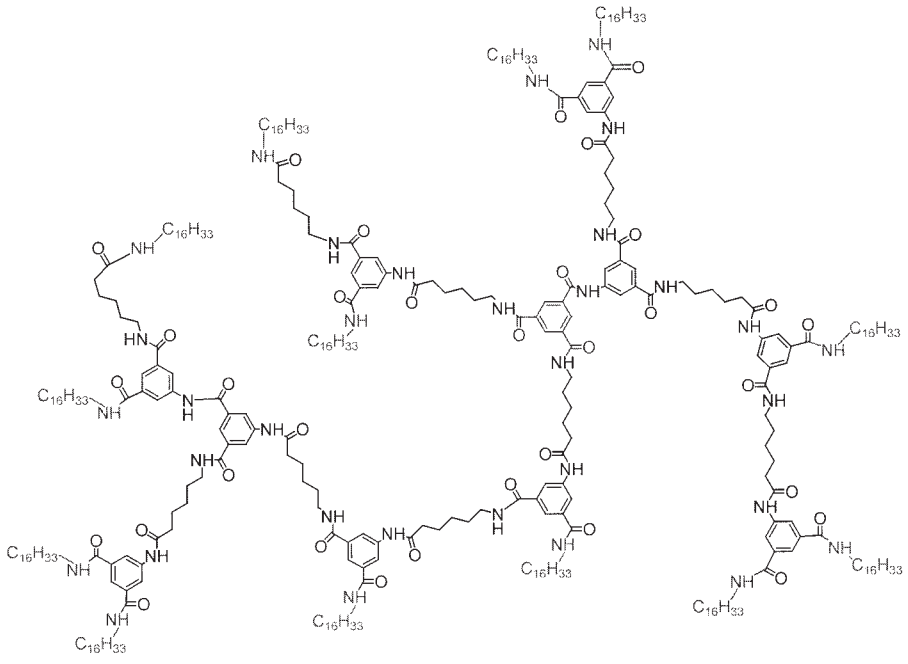

(b)

Figure 1 Structures of the amine-terminated (a) and the alkyl-terminated (b) hyperbranched (HB) aromatic polyamides prepared by a one-pot polymerization.

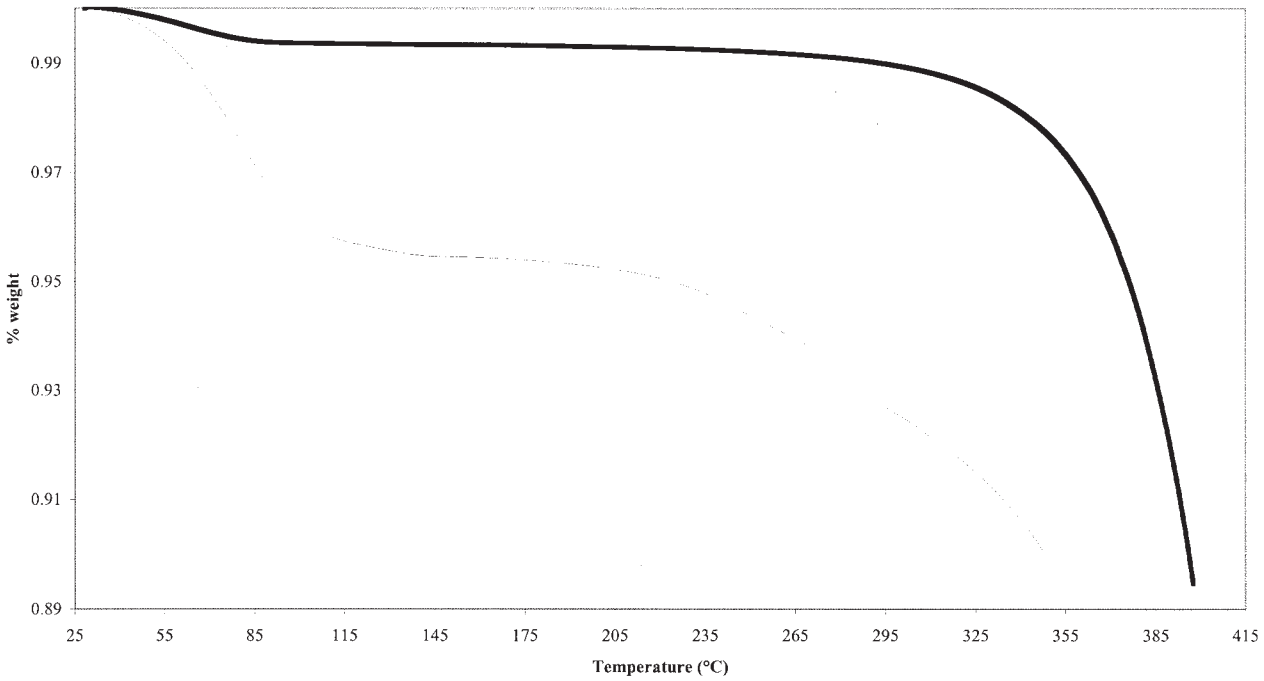

Figure 2 TGA runs for molecules A and B, showing the decomposition of each polymer. Thin line: Polymer A; thick line: Polymer B.

$$\varepsilon^* = \varepsilon_\infty + \frac{\varepsilon_r - \varepsilon_u}{[1 + (i\omega\tau_{HN})^{\alpha HN}]^{\beta HN}}$$

where ε_u is the unrelaxed permittivity, ε_r is the relaxed permittivity, ω is the angular frequency, τ_{HN} is the relaxation time, and α_{HN} and β_{HN} are the Havriliak–Negami distribution parameters.

To understand the molecular behavior of polar materials more fully, it is interesting to use the complex dielectric modulus formalism. The complex dielectric modulus is defined as follows: $M^* = M' + iM'' = 1/\varepsilon^*$, where $M' = \varepsilon'/(\varepsilon'^2 + \varepsilon''^2)$ and $M'' = \varepsilon''/(\varepsilon'^2 + \varepsilon''^2)$.

Dynamic mechanical analyses were performed using a DMA 2980 spectrometer (TA Instruments), which is used to determine storage modulus E', loss modulus E'', and tan δ ($=E''/E'$) in a temperature range from −150 to 220°C. All measurements were carried out between 1 and 50 Hz but only measurements at 10 Hz are presented in this work using isotherms every 3°C. Samples were dried before analysis at 110°C for 2 h *in situ*.

RESULTS AND DISCUSSION

Amine-terminated hyperbranched polymer (polymer A)

The TGA thermogram (see Fig. 2, thin line) shows the departure of an unknown compound, which is probably water, while heating (mass loss of 4.8%) between 50 and 100°C. This water release is found in the first DSC run (endothermic peak). The decomposition temperature of this polymer starts at 220°C. The second DSC run shows a glass transition at 104°C [see Fig. 3(a)]. Modulated DSC enabled separation of the glass-transition temperature and this endothermic peak resulting from release of water during the first run. Figure 4 shows the modulated heat flow and the deconvoluted baseline heat capacity. Glass transition was clearly apparent near 70°C. Global evolution of the heat flow in the range 50–150°C was endothermic, probably related to the water loss process.

Several dielectric experiments were carried out on a polymer A powder, as shown in Figure 5. The first run corresponds to heating between −140 and 220°C on an "as-received" powder and it shows, at 1 kHz, three relaxations comparable to those found in the polyamide-6,6[39]: a secondary relaxation, γ, attributed to the local chain movements at −90°C, is observed as well as another secondary relaxation, β, linked to the hydrogen-bond–type interactions between amide functions and water molecules at −30°C. The amplitude and the position of these relaxations are dependent on the polymer water content (e.g., the β-relaxation amplitude increases with increasing water content); this is clearly shown between the first and the second dielectric run because the polymer is drier during the second run than during the first run, which corresponds to heating again from −140 to 220°C. The principal relaxation α, associated with the glass transition of the polymer, is observed at 135°C (tan δ at 1

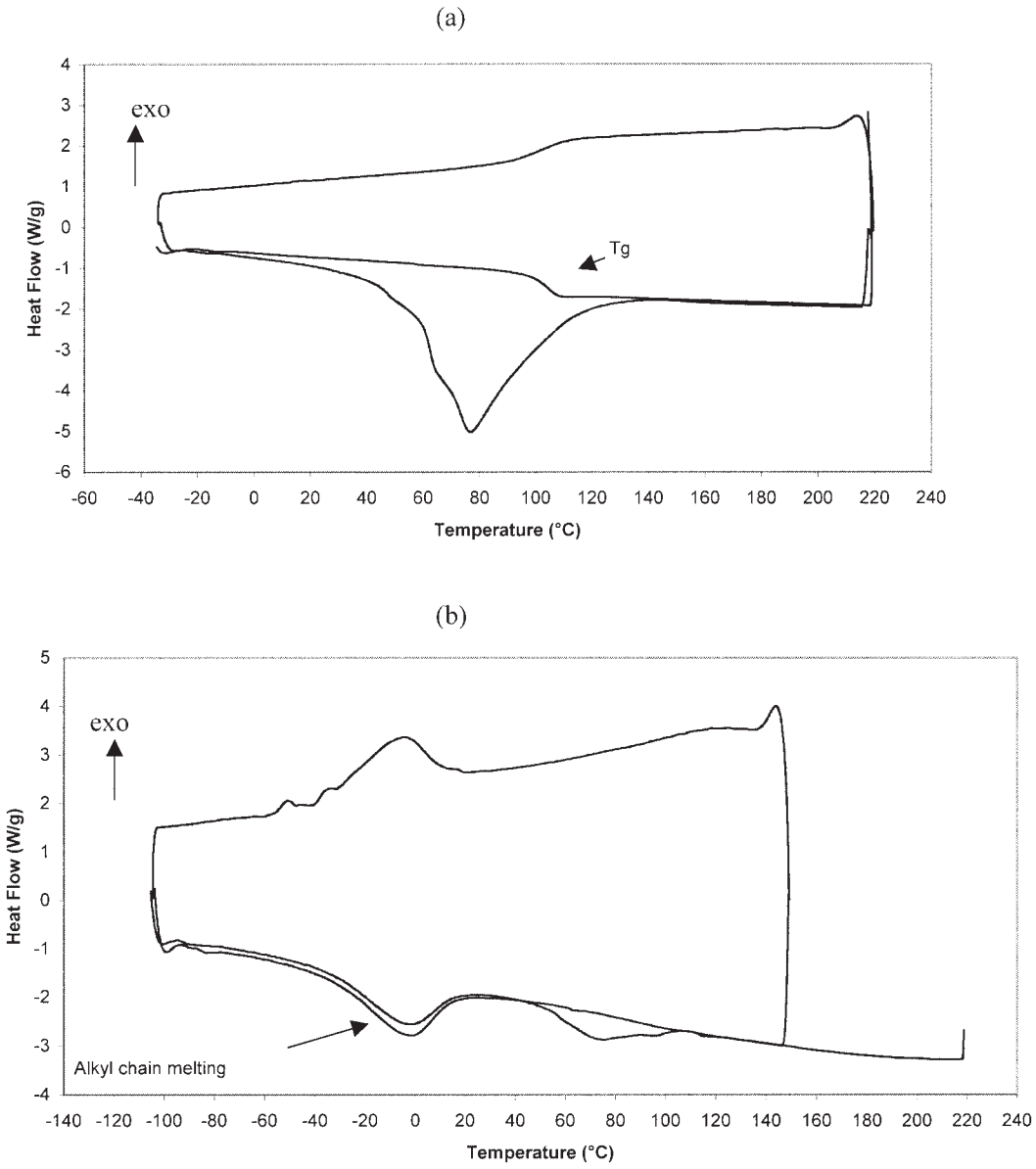

Figure 3 DSC thermograms of the HB amine-terminated (a) and alkyl-terminated (b) polyamides.

kHz) or can be seen at 150°C (dielectric modulus at 1 kHz) in Figure 6 on a dry sample. These results are in good agreement with the T_g value measured by DSC (104°C). At higher temperatures, an ionic relaxation linked to conduction and strongly frequency dependent was found, as can be seen in Figure 5 for 100 kHz. In addition, at 80°C a peak, which looks "independent of the frequency," is also shown in Figure 5. In fact, this frequency independence can be explained by the fact that the material is evolving with temperature and some water is released when the sample is heated in the dielectric cell, so in fact this water had "plastified" the system. This peak disappears in the second run and does not reappear significantly if the powder was humidified. This is not surprising because the T_g is higher than room temperature; so, because the system is in the glassy state, the water uptake is less likely to occur. This confirms the observations by DSC and the morphology modifications observed in the literature: even if the system does not recover the same water content that it had when it was "as received," the hypothesis that the unknown compound released in water is highly plausible.

Table I reports the positions of observed relaxations, their associated activation energies, and H.N. parameters (except for the α-relaxation, which was difficult to fit because it was convoluted with strong conduction). Activation energies were calculated under the assumption that secondary relaxations are associated with local movements using an Arrhenius-type equation:

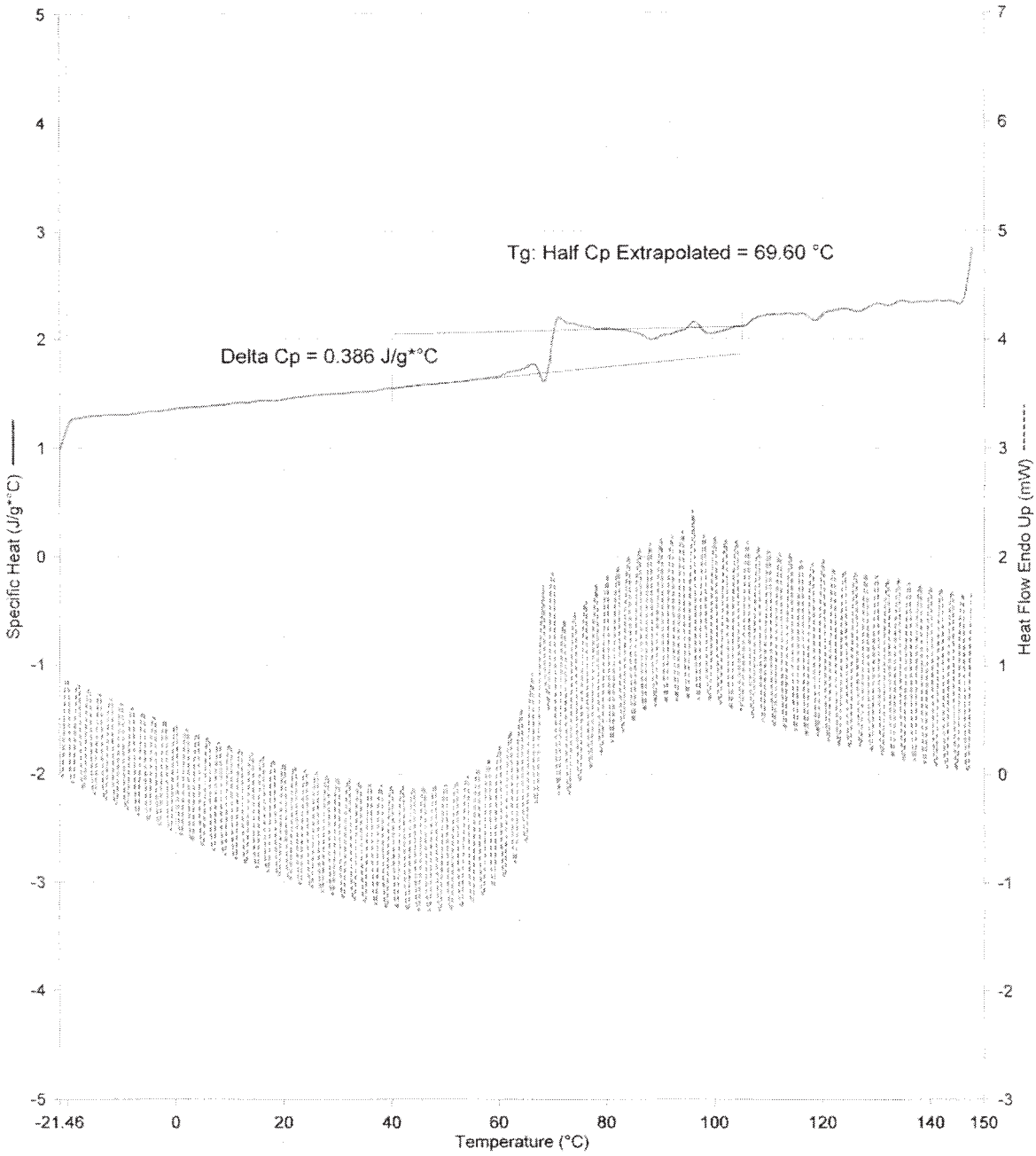

Figure 4 Modulated heat flow and deconvoluted baseline heat capacity for polymer A.

$$f_{max} = f_{\infty} \exp\left[-\frac{E_A}{\mathrm{kT}}\right]$$

Figure 6 represents an example of the H.N. fit obtained for β- and γ-relaxations. A good agreement can be observed between the experimental and fitted curves. The low values of activation energies found confirm that the corresponding relaxations are associated with local movements. As can be seen in Table I, β_{HN} parameters are close to 1, which shows that the two secondary relaxations (β and γ) have a Cole–Cole-type behavior ($\beta \approx 1$), which is characteristic of the symmetry of these dielectric relaxation peaks for the polymer A. It can be observed that the γ-relaxation has an even better symmetry than that of the β-relaxation. The increase of α_{HN} parameters for the β-relaxation from 0.3 to 0.5, compared to those of the γ-relaxations (0.2 to 0.3), can be explained by the fact that γ-relaxations give rise to more heterogeneous dipole motions than the β-relaxations. $\Delta\varepsilon_{\mathrm{HN}}$ parameters are globally higher for the β-relaxation than for the γ-relaxation in polymer A. $\Delta\varepsilon_{\mathrm{HN}}$ is linked to the amplitude of the dielectric relaxation, and thus more dipoles are participating in the β-relaxation than in the γ-relaxation.

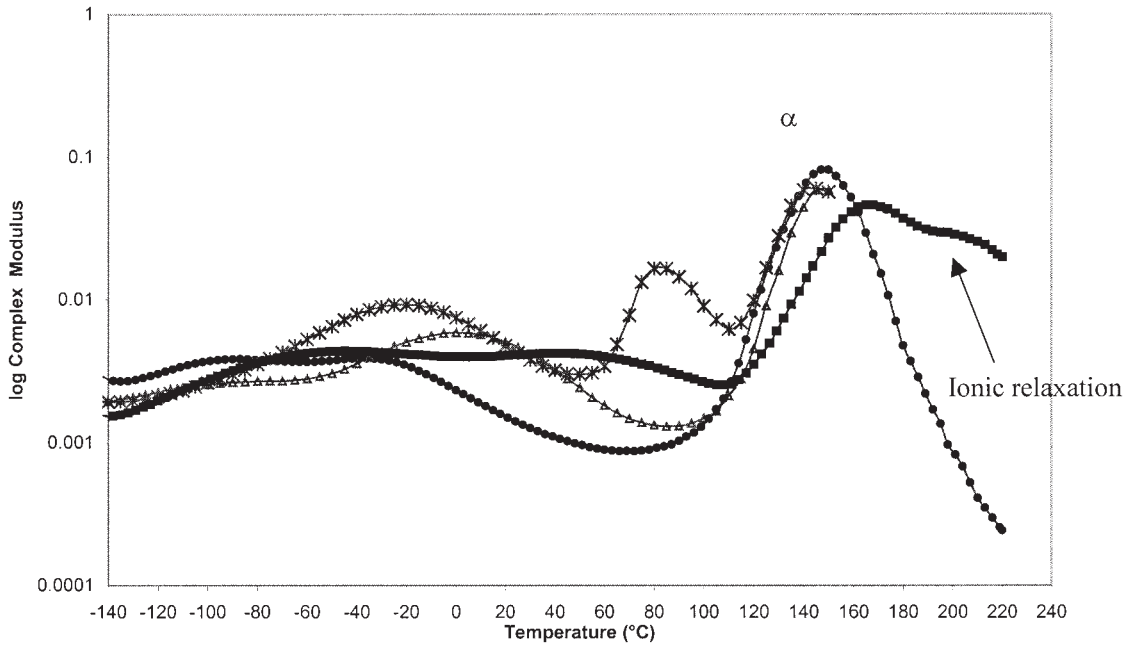

Figure 5 Dielectric modulus versus temperature at 1 kHz (●) and 100 kHz (■) for dried, humidified 2 days (△), and nondried as-received (×) amine-terminated HB. This figure also shows the β-relaxation dependency of water content.

Relaxation positions are given at 1 kHz using the dielectric modulus and the frequency range from 0.1 Hz to 10 MHz. Primary relaxation activation energies are difficult to calculate because of the presence of ionic conduction phenomena at high temperatures.

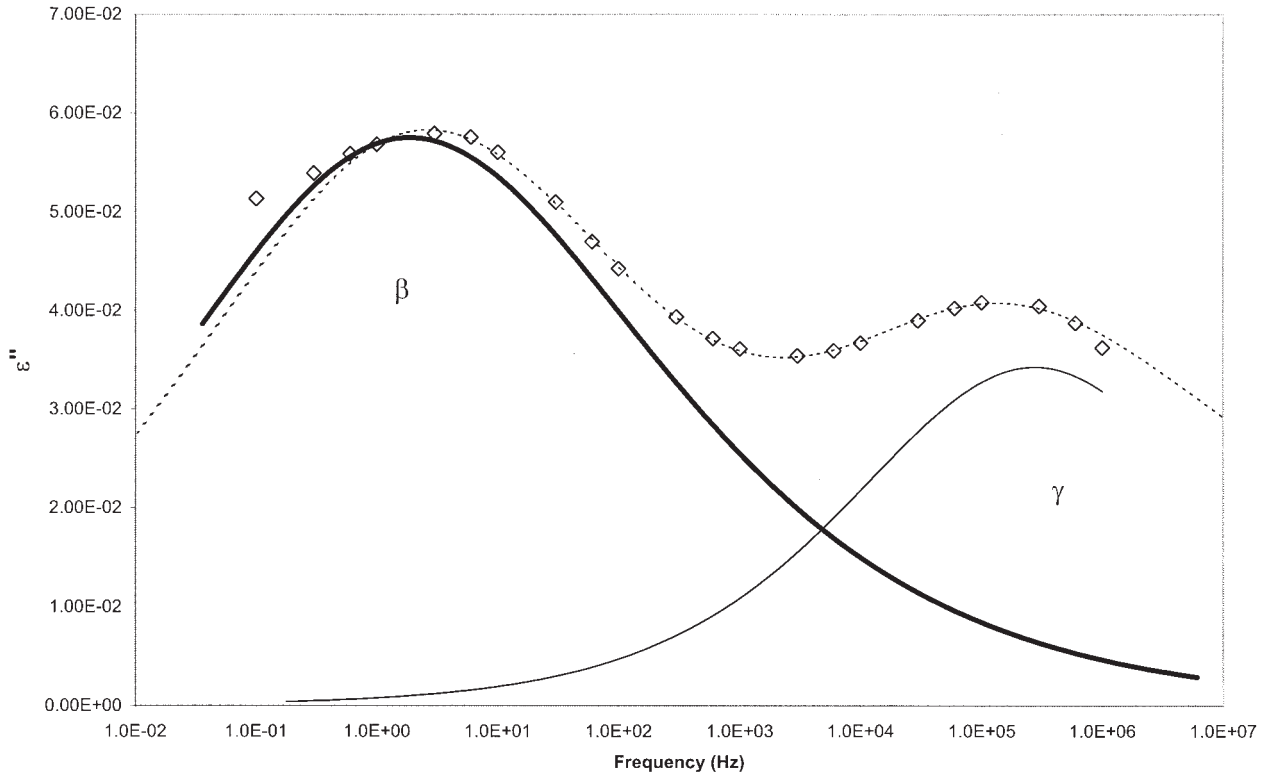

Figure 6 Examples of H.N. fits done on β-relaxation (thick line) and γ-relaxation (thin line) in the case of polymer D (PA-6,6 + 2% HB amine terminated) compared to the experimental points (◇) ε″ as a function of frequency and the total fit curve (- - -).

TABLE I
Positions of Maximum of tan δ at 1 kHz (±1°C), Activation Energies (±5 kJ/mol), and Havriliak–Negami (HN) α_{HN} and β_{HN} Parameters of Secondary Relaxations in Polymer A Measured Between −30 and +30°C for the β-Relaxation and Between −110 and 70°C for the γ-Relaxation

Polymer A	E_a (Temperature)	α_{HN}	β_{HN}	τ_{HN}[a]	$\Delta\varepsilon_{HN}$[a]
β-relaxation	55 kJ/mol (−30°C)	0.3–0.5	0.74–1	1.62×10^{-5}	0.21
γ-relaxation	31 kJ/mol (−90°C)	0.2–0.3	0.98–1	5.7×10^{-5}	0.18

[a] τ_{HN} (in s) and $\Delta\varepsilon_{HN}$ are given at −95 and 0°C, respectively.

Alkyl-terminated hyperbranched polymer (polymer B)

Measurements by TGA reveal a much lower weight loss (0.5%) than that previously observed between 50 and 120°C, relative to the absence, in the chain ends, of amine groups in interaction with water molecules (see Fig. 2, thick line). This means that the presence of water scarcely affects these polymer properties. The decomposition of this polymer is observed from 330°C. The DSC thermogram, shown in Figure 3(b), exhibits at −4°C, while heating, a melting of organized regions of terminal alkyl chains. Glass transition is not detected in the observed temperature domain.

Dielectric runs, carried out on polymer B (see Fig. 7), show the same relaxations but with a shape that is slightly different from that observed in polyamide-6,6 and in polymer A, that is, γ, β, and α (120°C at 1 kHz, complex dielectric modulus maximum), with an additional ionic relaxation at higher temperature, and confirm the TGA results as well as polymer independency on water content, which was not the case for polymer A.

After curve-fitting by a Havriliak–Negami-type equation (see an example of obtained fits in Fig. 6), activation energies were calculated using an Arrhenius-type equation. Table II details the positions of observed relaxations, their associated activation energies, and their H.N. parameters (except for the α-relaxation, which was difficult to fit because it was convoluted with strong conduction). The low values of activation energies found confirm that the corresponding relaxations are associated with local movements. As can be seen in Table II, β_{HN} parameters are close to 1, which shows that the two secondary relaxations (β and γ) have a Cole–Cole-type behavior ($\beta \approx 1$), which is characteristic of the symmetry of these dielectric relaxation peaks and is similar to the behavior of polymer A. Again, it can be observed that the γ-relaxation has a better symmetry than that of β-relaxation because this latter relaxation is more strongly influenced by the α-relaxation. The slight increase of α_{HN} parameters for the β-relaxation from 0.3 to 0.5, compared to those of the γ-relaxations (0.3 to 0.4), can be explained by the fact that γ-relaxations generate slightly more heterogeneous dipole motions than the β-relaxations (as in the case of polymer A). $\Delta\varepsilon_{HN}$ parameters are globally higher for the β-relaxation

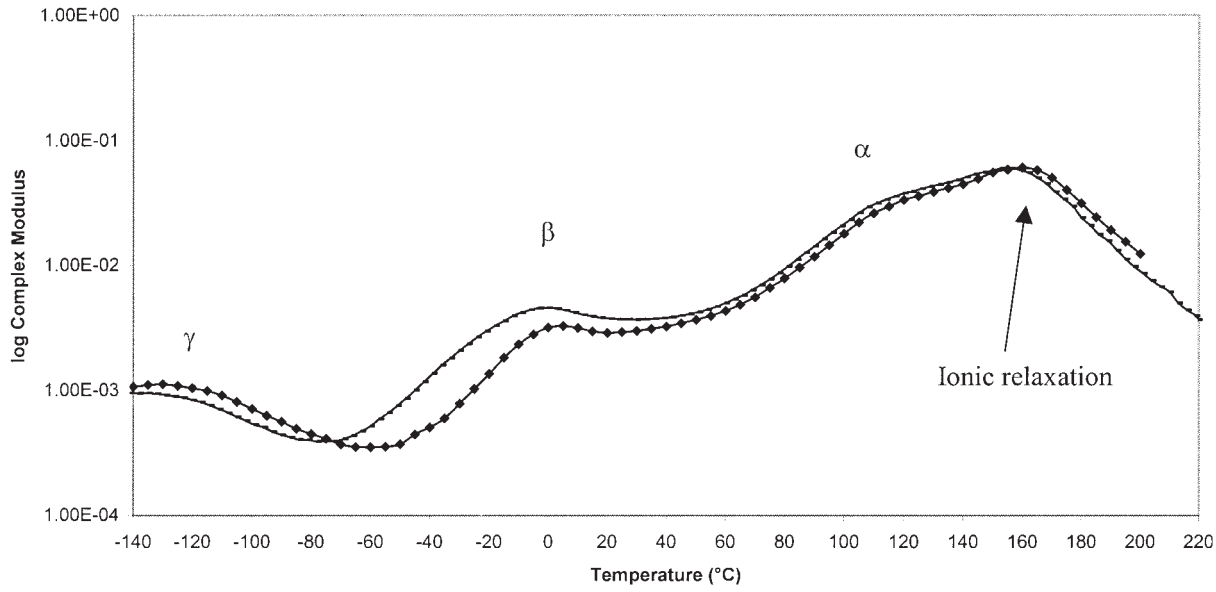

Figure 7 First (—) and second (◆) dielectric runs, Modulus versus frequency of the alkyl-terminated HB (polymer B) at 1 kHz.

TABLE II
Positions of Maximum of tan δ at 1 kHz (±1°C), Activation Energies (±5 kJ/mol), and Havriliak–Negami (HN) α_{HN} and β_{HN} Parameters of Secondary Relaxations in Polymer B Measured Between −30 and +30°C for the β-Relaxation and Between −110 and 70°C for the γ-Relaxation

Polymer B	E_a (Temperature)	α_{HN}	β_{HN}	τ_{HN}[a]	$\Delta\varepsilon_{HN}$[a]
β-relaxation	50 kJ/mol (0°C)	0.32–0.48	0.87–1	4.9×10^{-5}	0.11
γ-relaxation	25 kJ/mol (−120°C)	0.3–0.42	0.94–1	9.35×10^{-7}	0.021

[a] τ_{HN} (in s) and $\Delta\varepsilon_{HN}$ are given at −95 and 0°C, respectively.

than for the γ-relaxation in polymer B, as in the case of polymer B for the same reasons.

Blends of polyamide-6,6 with hyperbranched molecules

Polyamide-6,6 containing amine-terminated polymers (C, D, and E)

DSC measurements were performed on dried films at 10°C/min. Results can be found in Table III and show that the glass-transition temperature shifts to higher values when the percentage of hyperbranched polyamide increases in the blend, a phenomenon attributed to the higher T_g of hyperbranched polyamide (104°C) compared to the T_g of polyamide-6,6, which is around 52°C. It was verified that the T_g for the blend follows Fox's law [$1/T_g$ (blend) = $1/T_g$ (PA-6,6) + $1/T_g$ (HB amine terminated)]. This confirms that the amine-terminated hyperbranched polyamide is miscible into polyamide-6,6 (only one T_g was observed for the 2 and 5% blends). Moreover, TEM observations did not show any phase separation (see Fig. 8). The addition of this hyperbranched polyamide to the polyamide matrix does not seem to have any significant effect on the polyamide crystallinity ratio apart from slightly decreasing its value.

Dielectric relaxation studies on dried polyamide (polymer C) confirm the existence of all polyamide relaxations described in the literature.[40] At 1 kHz, the α-relaxation, with respect to T_g, is observed at about 100°C; the secondary relaxation β, attributed to hydrogen-type interactions between amide groups and water molecules, is located at −10°C; and the γ-relaxation is observed at −90°C. This relaxation is related to local chain movements. Finally, another relaxation is also observed at higher temperatures (at about 130°C) and can be related to the ionic conduction relaxation present in this temperature range.

For nondried polyamide, dielectric measurements reveal that the primary relaxation is 40°C lower than previous results, thus confirming the plasticizing effect of water. The β-relaxation is also more intense, with respect to the presence of water. The decrease of the real part of the complex modulus M' can be seen in Figure 9, which also reflects the same behavior.

Knowing the great similarity between the hyperbranched structure and the polyamide matrix, it is not obvious to detect the dielectric signal coming from the hyperbranched polymers in the blend, the quantity of

TABLE III
DSC Data on Pellets Obtained During the Second Run for Polymers C, D, E, F, and G

Parameter	C	D	E	F	G
T_m	263	260	260	262	262
ΔH_m (±2 J/g)	74	68	68	65	62
T_c	233	229	228	234	234
T_g midpoint (±2°C)	60	59	65	58	58
% of crystallinity	28.7%	28%	29.5%	26.7%	26.8%

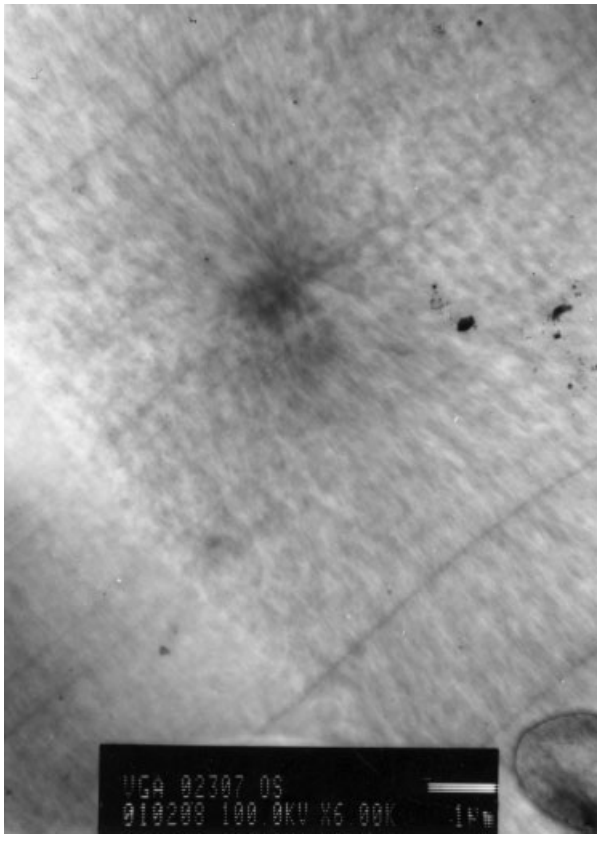

Figure 8 TEM micrograph of ultrathin sections of polymer D using OsO_4 staining technique.

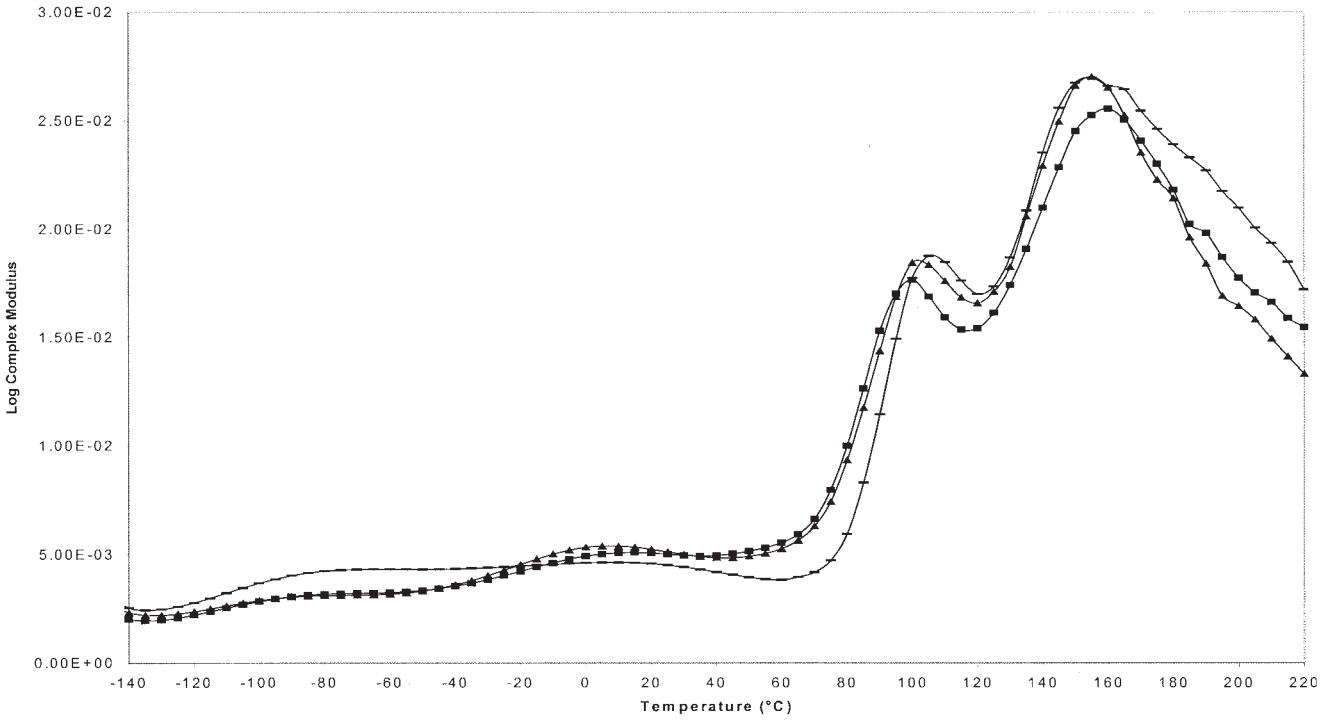

Figure 9 DRS results showing dielectric modulus versus temperature at 1 kHz for the polyamide-6,6 reference (polymer C) (■) and the blends with HB amine terminated (2%): D (▲) and (5%) E (—).

which was very small as well (2 and 5%). Therefore, as expected, the dielectric observations on polyamide blends (polymers D and E) do not show a multiplicity of peaks suitable to each blend entity. As in pure polyamide, three relaxation phenomena are observed, with some slight changes on the temperature position of the relaxations (no more than 5°C). These relaxations are shown in Figure 9. Table IV compares, at 1 kHz, the temperature peak positions for the three samples under investigation.

The increase of the α-relaxation temperature can be explained by a decrease in the amorphous-phase molecular mobility related to the addition of the amine-terminated hyperbranched polyamide, which can in turn hinder the motion of the main chains and develop some new interactions arising, for example, from hydrogen bonding. Finally, T_α values, which are more precisely obtained from dielectric measurements, confirm the tendency observed with the evolution of glass-transition values obtained from DSC measurements.

TABLE IV
DRS Results from Polymer Blends C, D, and E[a]

Relaxation	E_a (Temperature)	α_{HN}	β_{HN}	τ_{HN}	$\Delta\varepsilon_{HN}$
		Polymer C			
α	— (100°C)	—	—	—	—
β	73 kJ/mol (10°C)	0.28–0.45	0.90–1	3.57×10^{-4}	0.53
γ	35 kJ/mol (−90°C)	0.22–0.35	0.98–1	2.55×10^{-4}	0.28
		Polymer D			
α	— (105°C)	—	—	—	—
β	73 kJ/mol (10°C)	0.30–0.55	0.88–1	7.69×10^{-5}	0.76
γ	30 kJ/mol (−90°C)	0.25–0.35	0.99–1	2.83×10^{-5}	0.14
		Polymer E			
α	— (109°C)	—	—	—	—
β	75 kJ/mol (10°C)	0.33–0.60	0.85–1	6.86×10^{-5}	0.78
γ	26 kJ/mol (−85°C)	0.25–0.35	0.97–1	2.16×10^{-5}	0.14

[a] Temperature positions of the relaxations at 1 kHz (±1°C), activation energies (±5 kJ/mol), and HN parameters over the range of temperature where each relaxation occurs, that is: β, −30 to 30°C and γ, −110 to 60°C. τ_{HN} (in s) and $\Delta\varepsilon_{HN}$ are given at −95 and 0°C, respectively.

—, not measurable.

In conclusion, from the study of secondary relaxations, it is difficult to confirm any influence of this hyperbranched additive in the polyamide blend because the relaxation peaks are strongly convoluted. This is confirmed by the analysis of relaxation activation energies that vary only slightly. Table IV summarizes the value of activation energies (E_a) and the H.N. parameters for polymers C, D, and E (except for the α-relaxation, which was difficult to fit because it was convoluted with strong conduction). The E_a values are characteristic of local motions, as expected, but the values found for the β-relaxation are slightly higher than those found for the γ-relaxation.

As can be seen from Table IV, first the β_{HN} parameter is close to 1, meaning that the two secondary relaxations (β and γ) have a Cole–Cole-type behavior ($\beta \approx 1$), which is characteristic of the symmetry of these dielectric relaxation peaks and is similar to the behavior of polymers A and B. Again, it can be observed that the γ-relaxation has a better symmetry than that of the β-relaxation.

Second, mainly for the β-relaxation but slightly true for the γ-relaxation, the α_{HN} parameter increases with temperature, which means that the breadth of the distribution of relaxation times or the cooperativity decreases with temperature, which was the case for polymers A and B and is also true for polymers C, D, and E. Thus the motions of the dipoles associated with this relaxation process are more homogeneous. The increase of α_{HN} parameters for the β-relaxation from 0.3 to 0.6, compared to those of the γ-relaxations (0.2 to 0.3), can be explained by the fact that γ-relaxations generate more heterogeneous dipole motions than the β-relaxations (as in the case of polymers A and B). When comparing the α_{HN} parameters of polymer C (polyamide-6,6 reference) with those of the HB blends (D and E), it can be observed that the range of values for β- and γ-relaxations is slightly higher, which indicates a decrease of the cooperativity of the motions and which means that the dipole motions associated with these two relaxation processes are more homogeneous for polymers D and E than those for the polyamide-6,6 reference. This fact again supports the idea of a decrease of molecular mobility in the blends induced by the introduction of hyperbranched polymers in the polyamide matrix.

Polyamide-6,6 containing alkyl-terminated polymers (F and G)

DSC measurements performed on dried pellets are detailed in Table III. The melting and crystallization temperatures are almost similar between C, D, and E (within measurement errors). The glass-transition temperature increases by 5°C and the crystallinity ratio remains almost constant between the polyamide reference and the two blends.

Contrary to the previous case, a TEM micrograph of polymer F, shown in Figure 10, shows that the introduction of hyperbanched molecules in the polyamide matrix is characterized by the appearance of nodules, which are a few nanometers in diameter, thus confirming that this type of hyperbranched polyamide is not miscible in the polyamide-6,6 matrix. These TEM observations were performed on ultrathin sections (80 nm thick) obtained with an ultramicrotome. Before observations, the sections were OsO_4 stained. This phase separation may induce some interfacial polarization that could be detected by dielectric spectroscopy. On the other hand, dielectric spectra show the same relaxations as in the polyamide-6,6 reference with temperature positions and activation energies independent of the content of alkyl-terminated hyperbranched polymer in the blend (see Table V). This fact is another indication of the noninteraction between these polymers. It can be noticed that the evolution of the amplitude of the ionic conduction phenomenon at high temperature, which was not seen for the amine-terminated HB system, could also be an indication of phase separation. The temperature positions of the relaxation peaks, the corresponding activation energies, and the H.N. parameters (except for the α-relaxation, which was difficult to fit because it was convoluted with strong conduction) are listed in Table V. The activations energies are high for the α-relaxation, as expected, because it is associated with cooperative motions and is of the same order of magnitude as that for polymers D and E for the β- and γ-relaxations. As can be seen in Table V, the behavior of the α_{HN} and β_{HN} parameters is similar to that of polymers D and E concerning the β- and γ-relaxations. Finally, the τ_{HN} and $\Delta\varepsilon_{HN}$ parameters are globally higher for the β-relaxation than for the γ-relaxation in polymers C, D, E, F, and G, as was the case for polymers A and B. The τ_{HN} parameters of the β-relaxation are higher than those of the γ-relaxation, meaning that the motions involved in the β-relaxation process take longer to relax than those involved in the γ-relaxation process, as expected, except for polymers A and B for which the contrary is observed.

Comparison can be made also between the τ_{HN} of the β- and γ-relaxations compared to the polyamide reference (polymer C): a decrease of τ_{HN} values can be observed, which indicates a decrease of the temperature peak position of these relaxations for the polymers that contain the hyperbranched systems (with respect to the reference), contrary to the α-relaxation temperature variation observed.

Viscoelasticity measurements using the tensile mode were carried out to confirm dielectric results. The films of blends used are similar to those prepared for DRS. The obtained results (see Fig. 11) are similar to those observed by DRS: two secondary relaxations and a primary relaxation α. Table VI shows, respec-

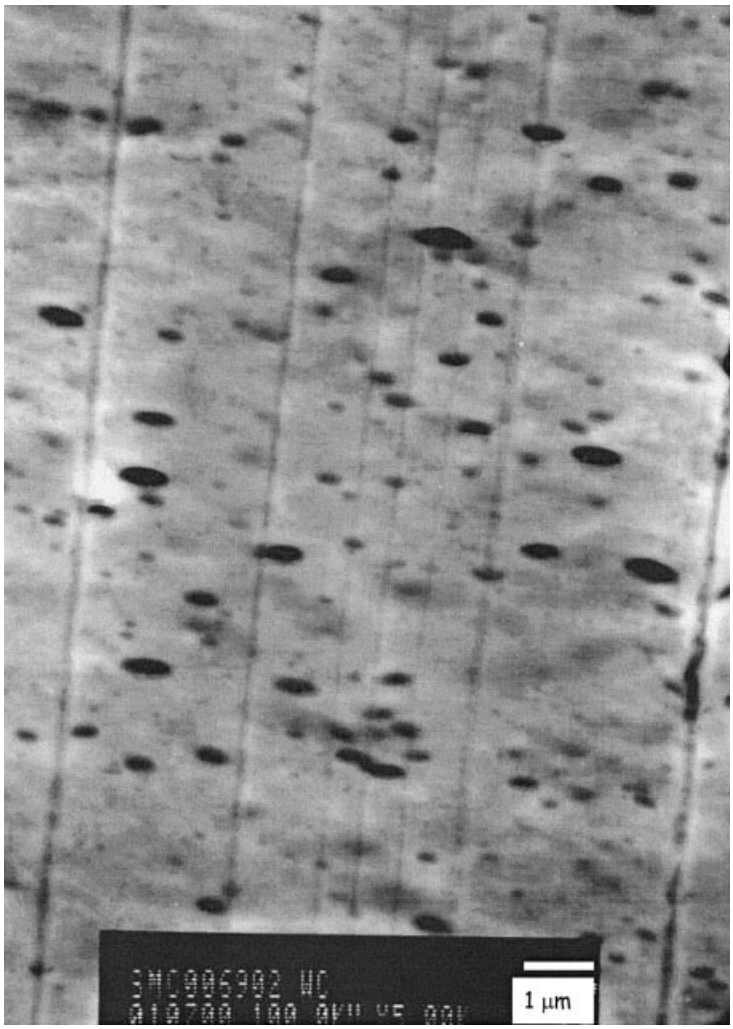

Figure 10 TEM micrograph of ultrathin sections of polymer F using the OsO_4 staining technique.

tively, the relaxation position at 10 Hz and the associated activation energies. The α-relaxation temperature is shifted to higher values for the amine-terminated blend as shown previously by DRS. It can be observed that the primary relaxation activation energy is difficult to calculate using this technique because of the limited number of frequencies available (only six between 1 and 50 Hz). Also shown in the dielectric spectra, the β-relaxation amplitude and its position vary enormously as a function of polyamide water

TABLE V
DRS Results from Polymer Blends F and G[a]

Relaxation	E_a (Temperature)	α_{HN}	β_{HN}	τ_{HN}	$\Delta\varepsilon_{HN}$
		Polymer F			
α	534 kJ/mol (101°C)	—	—	—	—
β	76 kJ/mol (12°C)	0.32–0.50	0.95–1	3.55×10^{-4}	0.31
γ	36 kJ/mol (−95°C)	0.25–0.40	0.99–1	3×10^{-4}	0.18
		Polymer G			
α	515 kJ/mol (101°C)	—	—	—	—
β	72 kJ/mol (12°C)	0.31–0.55	0.93–1	2.93×10^{-5}	0.39
γ	39 kJ/mol (−95°C)	0.24–0.30	0.97–1	1.60×10^{-5}	0.07

[a] Temperature positions of the relaxations at 1 kHz (±1°C), activation energies (±5 kJ/mol), and HN parameters over the range of temperature where each relaxation occurs, that is: β, −30 to 30°C and γ, −110 to 60°C. τ_{HN} (in s) and $\Delta\varepsilon_{HN}$ are given at −95 and 0°C, respectively.

—, not measurable.

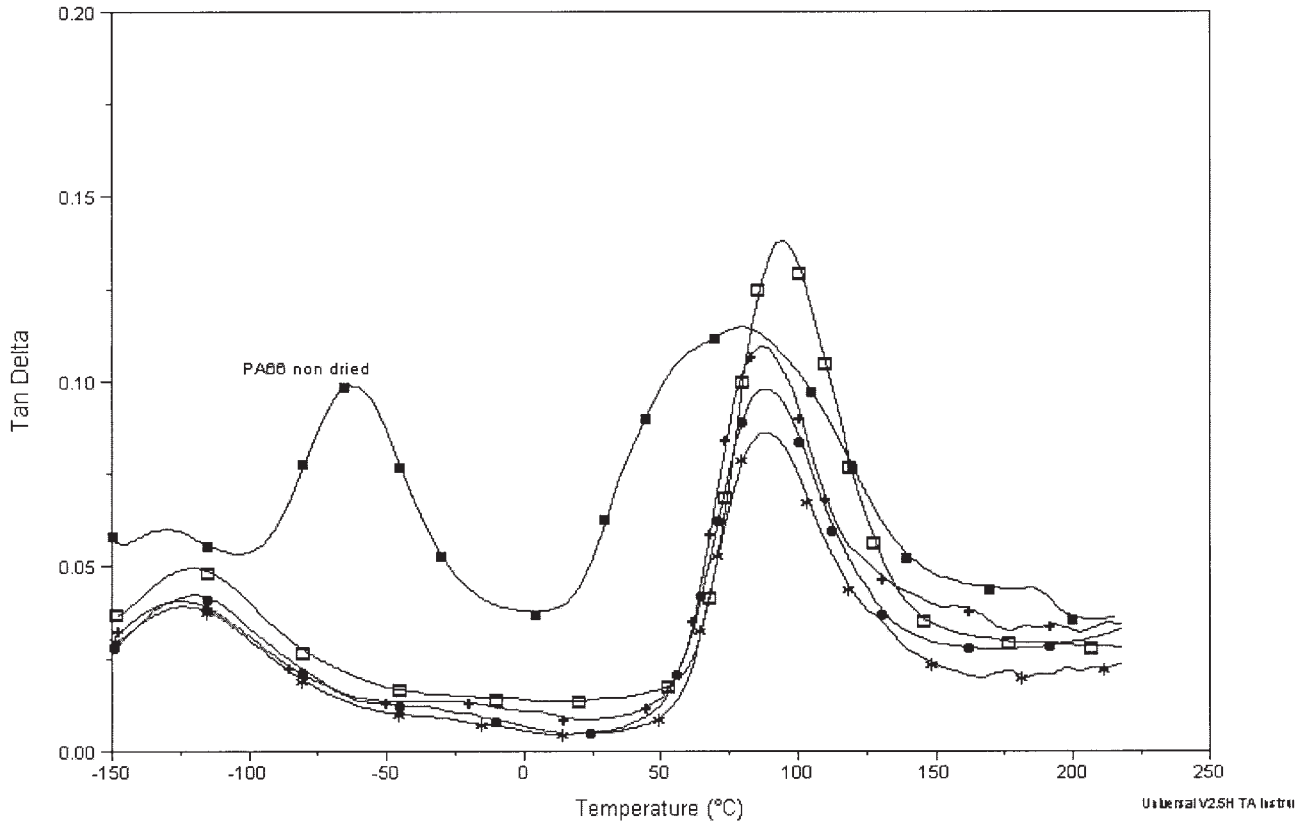

Figure 11 Viscoelastic analysis results showing tan δ (DMA) at 10 Hz for dried (●) and nondried (■) PA-6,6 (polymer C) and blends: E (□: 5% HB amine terminated), F (✚: 5% HB alkyl terminated), and G (*: 10% HB alkyl terminated).

percentage content. This relaxation, revealing the plasticizing role of water in the polyamide, is very intense in the nondried polyamide and practically nonexistent in the dried one. However, the β-relaxation is much more visible when looking at DRS measurements even on a dried sample because the interaction of –CONH– with traces of water can be very sensitively followed by this technique. Water is at the base of a local mobility increase followed by the rupture of a certain number of hydrogen bonds. The drying effect also modifies the α-relaxation, although it shifts to higher temperatures when the material is dried, thus confirming the DRS results. It can be observed as well from the viscoelastic results that the sample that has greater interaction with the matrix (5% HB amine terminated) has a higher α-relaxation amplitude than that of the dried polyamide-6,6 reference. Finally, a relaxation map can be found in Figure 12, which shows the variation of $\ln f_{max}$ as a function of $1/T$ and showing, through the slope of the straight lines observed for the β- and γ-relaxations, the evolution of the activation energies for polymer C and polymer blends E and F.

CONCLUSIONS

Thermal and dielectric properties of two kinds of hyperbranched polyamides were investigated, especially by DSC, TGA, and broadband dielectric spectroscopy. For both amine and alkyl-terminated polymers, pri-

TABLE VI
DDMA Results for Dried and Nondried PA-6,6 (Polymer C) and Polymer Blends E and G[a]

Relaxation	C nondried E_a (kJ/mol)	C dried E_a (kJ/mol)	E E_a (kJ/mol)	G E_a (kJ/mol)
	(Temperature)	(Temperature)	(Temperature)	(Temperature)
γ	40 (−128°C)	34 (−118°C)	38 (−124°C)	32 (−125°C)
β	85 (−63°C)	—	—	—
α	— (70°C)	— (83°C)	— (89°C)	— (89°C)

[a] Temperature positions of the relaxations given at 10 kHz (±1°C) and activation energies (±10 kJ/mol).

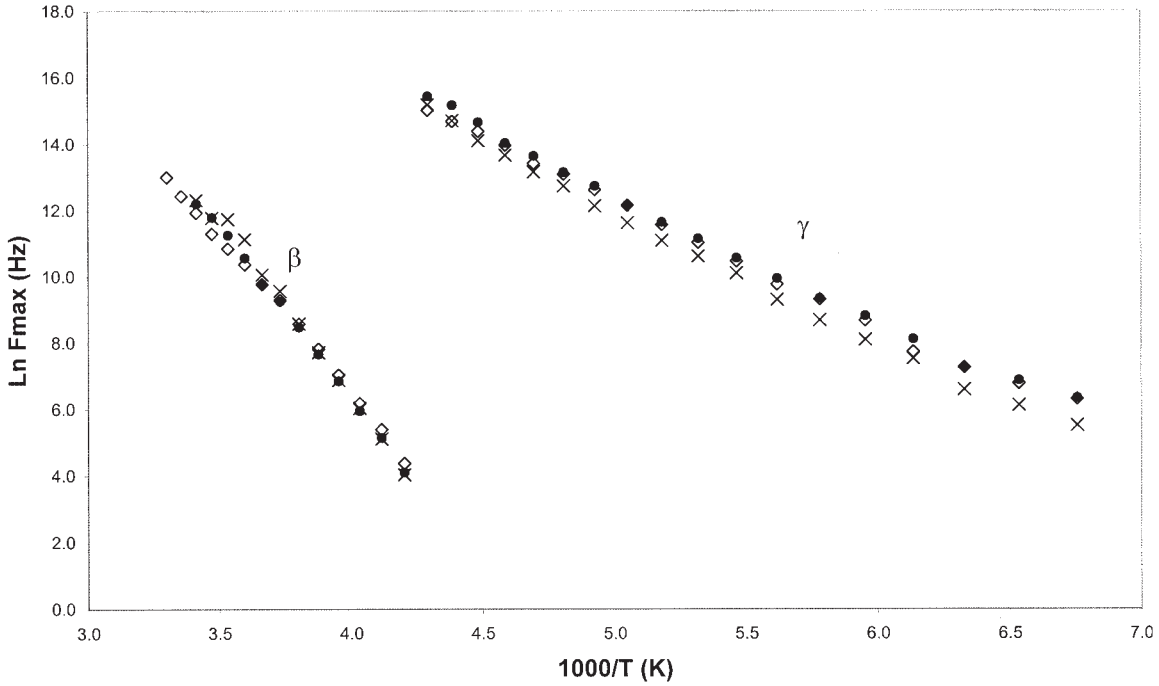

Figure 12 Relaxation map $\ln f_{max}$ (Hz) = $1/T$ for polymer C (◇), polymer E (×), and polymer F (●) in the case of the β- and γ-relaxations.

mary relaxations, with respect to the T_g, were observed at 80 and 110°C, respectively. Two secondary relaxations were also found and attributed. These relaxations are comparable to those observed in polyamide-6,6. The dielectrically determined glass-transition temperatures agree well with the thermally measured values, particularly for the amine-terminated polyamide. Infrared spectra confirmed the structure for each polymer and revealed a characteristic peak of the hyperbranched polyamide in both cases.

The objective of this work was the study of the interactions between polyamide-6,6 and hyperbranched polyamides with different terminations. The use of hyperbranched polymers, as additives, change some matrix properties to which these hyperbranched polymers are added. Thus, a decrease of relative permittivity value and an increase of glass-transition temperature were observed when the percentage of amine-terminated hyperbranched polyamide increased in the matrix. On the other hand, some other properties such as melting point and crystallization temperature remain practically independent of hyperbranched content. One of the noteworthy interests here is the ability to characterize the pure hyperbranched polymers in powder form by dielectric spectroscopy, which was a challenge at the beginning because a special powder cell had to be designed.

According to these studies, the amine-terminated polymer hinders the mobility of the polyamide chains. In the case of polyamide blend with the alkyl-terminated hyperbranched polymer, the results are indistinct from those of the polyamide-6,6.

The authors thank Rhodia St-Fons (CRL) for providing us with samples, for fruitful discussions, and for financial support. We also thank Dr. Olivier Gain (ISTIL) for help with the mechanical measurements, and Philippe Menez and Isabelle Bornard (CRL) for TEM characterizations.

References

1. Tomalia, D. A.; Naylor, A. M.; Goddar, W. A., III. Angew Chem Int Ed Engl 1990, 9, 138.
2. Fréchet, J. M. J. Science 1994, 63, 1710.
3. Fréchet, J. M. J.; Hawker, C. J.; Gitsov, I.; Leon, J. W. J Macromol Sci Pure Appl Chem 1996, A33, 1399.
4. Malmstrom, E.; Hult, A. J Macromol Sci Rev Macromol Chem Phys 1997, C37, 555.
5. Archut, A.; Vogtle, F. Chem Soc Rev 1998, 37, 2193.
6. Kim, Y. H. J Polym Sci Part A: Polym Chem 1998, 36, 1685.
7. Frey, H. Angew Chem Int Ed Engl 1998, 37, 2193.
8. Fisher, M.; Vogtle, F. Angew Chem Int Ed Engl 1999, 38, 884.
9. Yoshitaka, Y.; Mitsuru, U.; Kazuhiko, T.; Michihiko, A. Macromolecules 1999, 32, 8363.
10. Jikei, M.; Kakimoto, M.-A. Prog Polym Sci 2001, 26, 1233.
11. Holter, D.; Burgath, A.; Frey, H. Acta Polym 1997, 48, 30.
12. Kim, Y. H.; Webster, O. W. J Am Chem Soc 1990, 112, 4592.
13. Hawker, C. J.; Lee, R.; Fréchet, J. M. J. J Am Chem Soc 1991, 113, 4583.
14. Turner, S. R.; Voit, B. I.; Mourey, T. H. Macromolecules 1993, 26, 4617.
15. Turner, S. R.; Walter, F.; Voit, B. I.; Mourey, T. H. Macromolecules 1994, 27, 1611.
16. Huwe, A.; Appelhans, D.; Prigann, J.; Voit, B. I.; Kremer, F. Macromolecules 2000, 33, 3762.
17. Wooley, K. L.; Frechet, J. M. J.; Hawker, C. J. Polymer 1994, 35, 4489.
18. Kim, Y. H.; Beckerbauer, R. Macromolecules 1994, 27, 1968.
19. Wooley, K. L.; Hawker, C. J.; Pochan, J. M.; Frechet, J. M. J. Macromolecules 1993, 26, 1514.

20. Khadir, A.; Gauthier, M. In: Proceedings of SPE ANTEC'97—Saving Planet Earth, Toronto, Canada, April 27–May 2, 1997; p 3732.
21. Carr, P. L.; Davies, G. R.; Feast, W. J.; Stainton, N. M.; Ward, I. M. Polymer 1996, 37, 2395.
22. Mulkern, T.; Beck, J.; Tan, N. C. Polymer 2000, 41, 3193.
23. Wu, S. Polymer 1985, 26, 1855.
24. Simmons, A.; Baker, W. E. Polym Commun 1990, 31, 20.
25. Dharmarajan, N.; Datta, S.; Ver Strate, G.; Ban, L. Polymer 1995, 36, 3849.
26. Scott, C. E.; Macosko, C. W. Polym Eng Sci 1995, 35 1938.
27. Scott, C. E.; Macosko, C. W. Polymer 1994, 35, 5422.
28. Fowler, M. W.; Baker, W. E. Polym Eng Sci 1988, 28, 1427.
29. Malmstrom, E.; Liu, F.; Boyd, R. H.; Hult, A.; Gedde, U. W. Polymer 1997, 38, 4873.
30. Zhu, P. W.; Zheng, S.; Simon, G. Macromol Chem Phys 2001, 202, 3008.
31. Trahasch, B.; Frey, H.; Lorenz, K.; Stuhn, B. Colloid Polym Sci 1999, 277, 1186.
32. Trahasch, B.; Stuhn, B.; Frey, H.; Lorenz, K. Macromolecules 1999, 32 1962.
33. Emran, S. K.; Newkome, G. R.; Weis, D. W.; Harmon, J. P. J Polym Sci Part B: Polym Phys 1999, 37, 2025.
34. Vogel, H. Phys Z 1921, 22, 645.
35. Fulcher, G. S. J Am Chem Soc 1925, 8, 958.
36. Tammann, G.; Hesse, W. Z Anorg Allg Chem 1926, 156, 245.
37. Dantras, E.; Lacabanne, C.; Caminade, A. M.; Majoral, J. P. Macromolecules 2001, 34, 3808.
38. McCrum, N. G.; Read, B. E.; Wiliams, G. Anelastic and Dielectric Effects in Polymeric Solids; Wiley: London, 1967.
39. Hedvig, P. Dielectric Spectroscopy of Polymers; Adam Hilger: London, 1977.
40. Steeman, P. A. P.; Maurer F. H. J. Polymer 1992, 33, 4236.
41. Havriliak, S., Havriliak, S. J. In: Relaxation in High Molecular Weight Materials, Dielectric and Mechanical Relaxation in Materials: Analysis, Interpretation and Application to Polymers; Carl Hanser-Verlag: Munich/New York, 1997; Chapter 7, p 202.
42. Kremer, F.; Schönhals, A. In: Dielectric Properties of Inhomogeneous Media, Steeman, P. A. M.; van Turnhout, J., Eds.; Broadband Dielectric Spectroscopy, Springer-Verlag: Berlin/New York, 2002; Chapter 13, pp 512–513.
43. Baird, M. E.; Goldsworthy, G. T.; Creasy, C. J. Polymer 1971, 12, 159.
44. Rhodia Research. WO Pat. 03/051998, 2003.
45. Sassi, J. F.; Touraud, F.; Dubois, J.; Vergelati, C. PMSE 2001, 84, 782.
46. Advanced Thermal Analysis System. May be accessed at http://web.utk.edu/~athas/
47. Havriliak, S.; Negami, S. J Polym Sci Part C 1966, 14, 99.